Available online at www.sciencedirect.com
ScienceDirect
Journal of the European Ceramic Society 28 (2008) 2739–2745
www.elsevier.com/locate/jeurceramsoc

Formation of PZT crack-free thick films by electrohydrodynamic atomization deposition

D. Wang [a,*], M.J. Edirisinghe [b], R.A. Dorey [a]

[a] *Microsystems & Nanotechnology Centre, Cranfield University, Bedfordshire MK43 0AL, UK*
[b] *Department of Mechanical Engineering, University College London, London WC1E 7JE, UK*

Received 7 February 2008; received in revised form 27 March 2008; accepted 4 April 2008
Available online 2 June 2008

Abstract

In this work, electrohydrodynamic atomization was used to spray deposit lead zirconate titanate (PZT) thick films using a PZT composite sol–gel slurry. During atomization splats and clusters were generated from jet break-up. The influence of atomization–substrate distance on the characteristics of splats and clusters was analysed. At a greater distance dried clusters were predominant, which led to the formation of porous films; conversely, at a smaller distance wet splats dominated, which generated dense films. A distance of 10 mm was found to be the optimum deposition distance for this slurry to produce dense films. 28 μm thick PZT crack-free films were produced by depositing 60 layers of slurry using this technique. The resulting films had a homogenous microstructure and exhibited a relative permittivity of ∼ 220 and $d_{33,f}$ of ∼71 pC N^{-1}.

Keywords: PZT; Films; Suspensions; Electrohydrodynamic atomization

1. Introduction

It is well known that piezoelectric materials are able to transform signals between electrical and mechanical impulses via the piezoelectric effect, which has been widely used in applications such as sensors, actuators, transformers and transducers.[1–4] Lead zirconate titanate (PZT) is one of the most important piezoelectric materials due to its high piezoelectric constant, relative permittivity and electromechanical coupling coefficient.[5] PZT thick films between 10 and 100 μm thick are of great interest in micro-electromechanical system (MEMS) due to the drive for miniaturisation, high power/sensitivity and system integration.[6] However, because of the limitation of low deposition rates and propensity for stress generation during processing, thin film fabrication methods, such as physical vapour deposition (PVD) [e.g. sputtering and pulsed laser deposition (PLD)], chemical vapour deposition (CVD), present significant technical challenges for producing PZT thick films in this thickness range.[7] The use of conventional bulk ceramic processing with subsequent machining and bonding is wasteful of material and time consuming.[8] Other thick film fabrication techniques based on sintering of oxide ceramic particles, such as screen printing, require temperatures normally above 1200 °C, which are likely to damage substrates and electrodes.[9]

Using a combination of conventional sol–gel processing and PZT powder processing, referred to as composite film (ComFi) technology, thick films of 2–30 μm can be fabricated using spin-coating methods at lower temperatures.[10,11] However, cracking and out of plane bending are likely to be generated due to the high stresses produced during the infiltration process, which is needed to improve the density and piezoelectric property of the films.[12]

Electrohydrodynamic atomization (EHDA) deposition provides a new way for forming PZT thick films. EHDA makes use of electrical and mechanical forces to form a liquid jet and its further disintegration into droplets[13] and was first reported by Zeleny in 1914.[14] This phenomenon can be explained by the Rayleigh limit,[15] described by $Q_R = 2\pi(16\gamma\varepsilon_0 r^3)^{1/2}$ where Q_R is the Rayleigh limit charge on a drop, γ is the liquid surface tension, ε_0 is the permittivity of free space, and r is the drop radius. Fission of a highly charged drop takes place when Q_R is exceeded and the surface tension force is overcome. A metal capillary is usually used as an atomizer nozzle, and a plate, ring or point (positioned below the nozzle) serves as

* Corresponding author.
E-mail address: d.wang@cranfield.ac.uk (D. Wang).

0955-2219/$ – see front matter © 2008 Elsevier Ltd. All rights reserved.
doi:10.1016/j.jeurceramsoc.2008.04.013

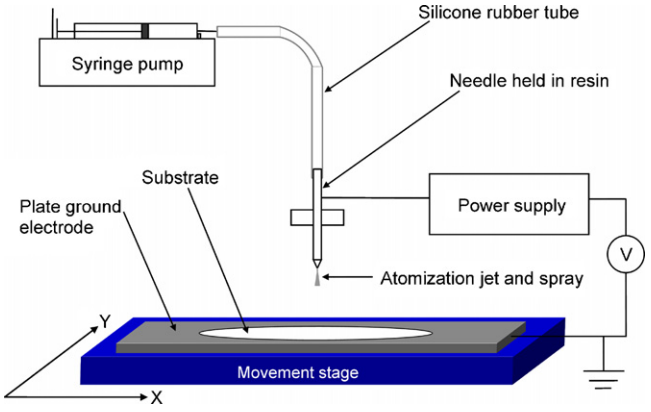

Fig. 1. Schematic representation of EHDA deposition equipment rig.

the ground electrode depending on the requirement of droplets motion.[16,17] According to the geometry of the jet and droplet, the resulting atomization modes can be mainly classified as dripping, microdripping, spindle, multi-spindle, cone-jet and multi-jet.[18] Among these the stable cone-jet mode is the most interesting functioning mode due to the production of small and uniform droplets. The investigations of EHDA using liquids are comprehensive,[19–21] but the use of suspensions is a more recent development.[16] The major advantage of this technique is its capability of forming small droplets.[22] The use of a suspension with this technique offers two distinct advantages: (a) fine deposition product and (b) less risk of nozzle blockage during processing as frequently observed with other droplet forming routes such as piezo-head drive ink-jet printing.[23] In this work a PZT composite sol–gel slurry was used with the EHDA technique enabling the formation of a wide range of PZT thick films for MEMS devices.

2. Experimental details

2.1. PZT sol

The PZT sol was prepared from the precursors lead acetate, titanium isopropoxide and zirconium propoxide. 3.55 g of titanium(IV) isopropoxide (99.99 wt.% purity) was added to 5.39 g of zirconium(IV) propoxide (76 wt.% in 1-propanol) prior to the addition of the solvents 1-propanol (99.7 wt.% purity, 5 ml) and glacial acetic acid (99.8 wt.% purity, 10 ml). An excess (9.95 g) of lead(II) acetate trihydrate was then added to the solution and the system was refluxed at a low heat for 30 min. The sol concentration was adjusted to 0.42 M by adding 13.2 ml of 1-propanol and 12 ml of acetic acid. The chemical stoichiometric ratio of the metal ions in the PZT sol was Pb 1.10:Zr 0.48: Ti 0.52.

2.2. PZT slurry

The composition of the PZT slurry is shown in Table 1. All the components were mixed in a nitrogen environment, then ball-mixed on a roller for 24 h. The PZT powder (PZ 26, Ferroperm, Denmark) has a mean particle size of ~0.6 μm. 2 wt.% of a

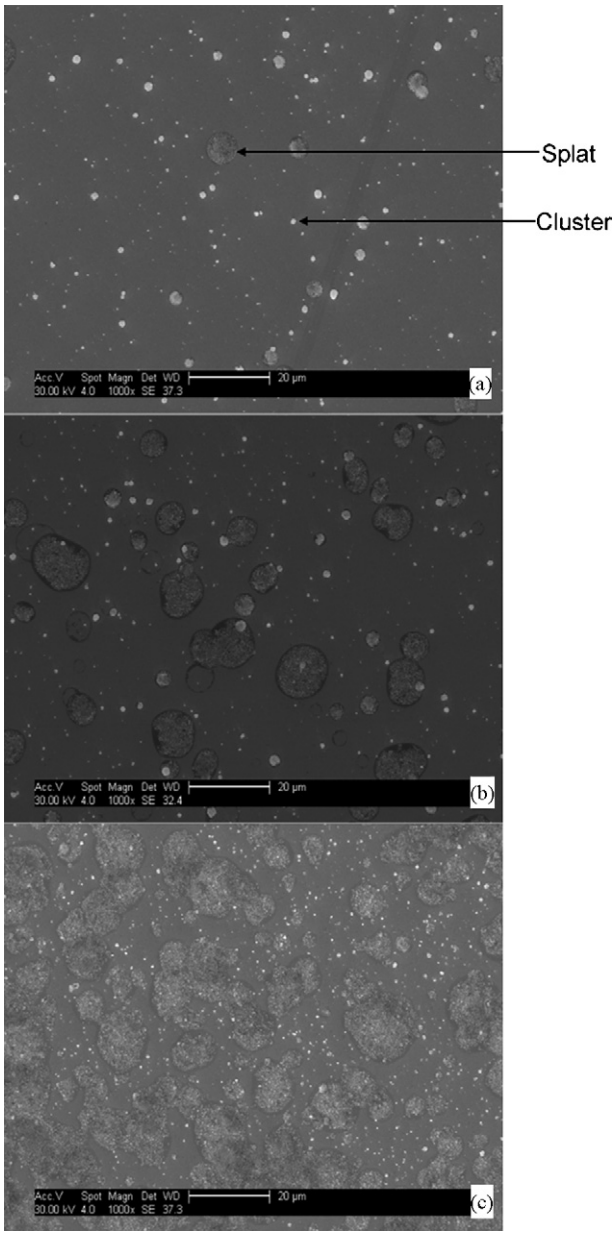

Fig. 2. Scanning electron microscope micrographs showing the one path deposition of PZT slurry at a flow rate of 2.2×10^{-10} m^3 s^{-1} and different working distances and applied voltages: (a) 20 mm and 7.5 kV, (b) 15 mm and 6.5 kV and (c) 10 mm and 5.5 kV.

dispersant KR 55 (Ken-React Lica 38, KenRich) was added to stabilize the slurry. The addition of 4.7 wt.% of Cu_2O–PbO sintering aid, with respect to the PZT powder, helps to increase the density and piezoelectric properties of the sintered PZT film.[24] This PZT slurry has the advantage of forming thick films at a low

Table 1
Composition of the PZT slurry using in the EHDA deposition process

PZT powder	10 g
PZT sol	14.2 ml
Sintering aid Cu_2O/PbO	0.069/0.428 g
Dispersant KR55	0.2 g
Zirconia ball-milling media	100 g

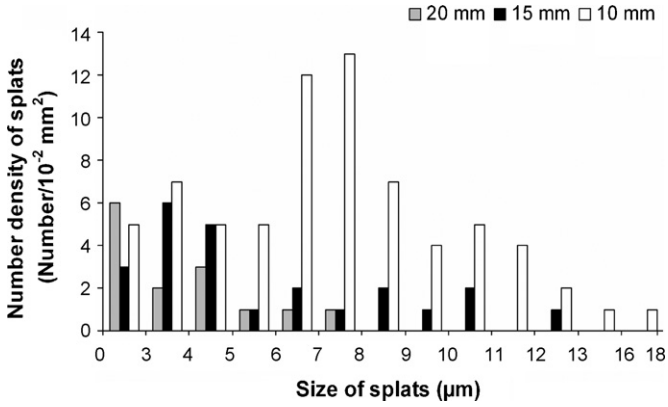

Fig. 3. The influence of working distance on splat size and density for PZT films deposited using EHDA deposition employing working distances of 20 mm, 15 mm and 10 mm.

processing temperature due to the presence of nanoscale particles in the sol inducing a high densification driving force.[25] The PZT slurry was ball-milled again for 2 h just before deposition to ensure throughout mixing.

2.3. Deposition of PZT slurry

The EHDA deposition device is shown in Fig. 1, and comprises of an electrohydrodynamic needle coupled together with a computer controlled *X–Y* movement stage. The needle, with inner/outer diameter of 0.85/1.3 mm, was connected to a high voltage power supply and its inlet was connected to a syringe pump using a silicone rubber tube through which PZT slurry was pumped. A high voltage power supply (Glassman High Voltage Inc., NJ, USA) was used to apply an electric field between the needle and the ground electrode, and a syringe pump (KD Scientific Inc., MA, USA) was employed to provide the hydrodynamic force to push the PZT slurry up to the outlet of the needle. A thin aluminium plate, serving as the ground electrode, was placed directly on the *X–Y* movement stage and connected to earth potential.

The substrate, a 25 mm × 25 mm silicon wafer, coated with Ti/Pt (8/100 nm) deposited using RF magnetron sputtering

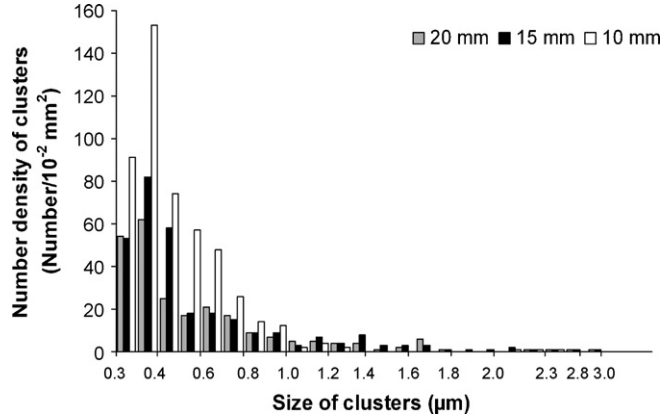

Fig. 4. The influence of working distance on cluster size and density for PZT films deposited using EHDA deposition employing working distances of 20 mm, 15 mm and 10 mm.

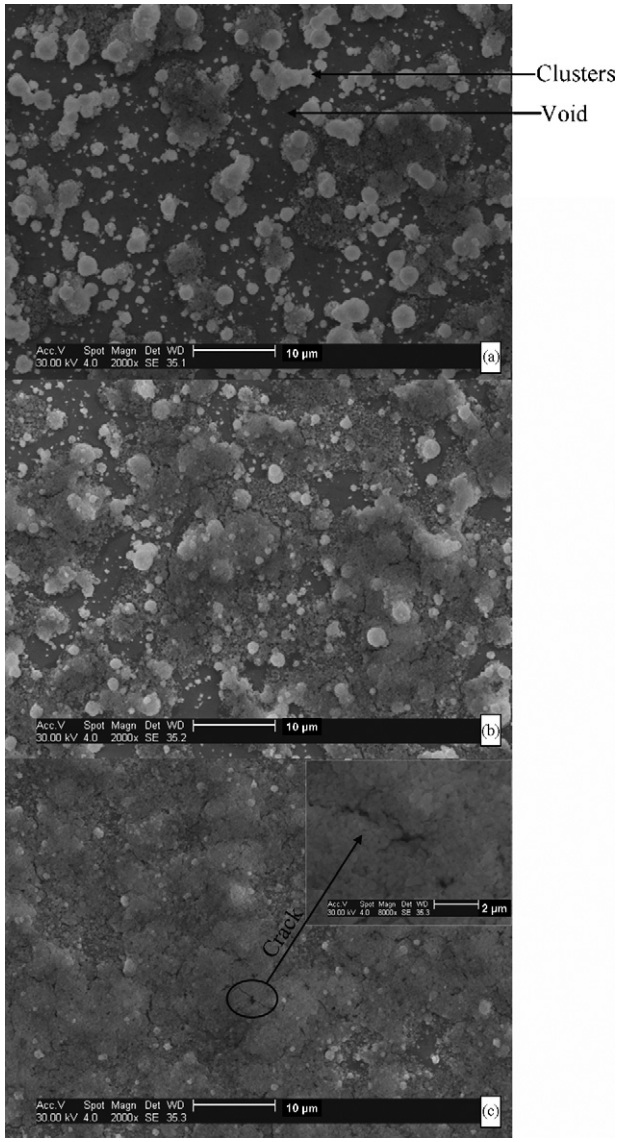

Fig. 5. Scanning electron microscope micrographs showing the one layer of PZT slurry deposited at a flow rate of 2.2×10^{-10} m^3 s^{-1} and different atomization distances and applied voltages: (a) 20 mm and 7.5 kV, (b) 15 mm and 6.5 kV and (c) 10 mm and 5.5 kV.

(Nordiko Ltd., Hampshire, UK), was placed on the aluminium plate ground electrode and kept at a fixed distance from the needle throughout deposition. During the formation of the PZT films the substrate was alternately rastered with the major scan in the *X* and *Y* directions with a speed of 30 mm s^{-1} to build up the film. The distance between two neighbouring parallel paths of deposition was set to 3.6 mm to ensure a degree of overlap between deposited material.

After every two intermediate layer depositions (one *X* direction scan and one *Y* direction scan) the PZT film was dried at 200 °C for 60 s and pyrolysed at 350 °C for 60 s using a hotplate to remove all the organic components. The final film was sintered at 720 °C for 20 min in a muffle furnace. A chromium/gold top electrode with a thickness of 15/100 nm and a diameter of 2 mm was deposited by vacuum evaporation (Edwards Evaporator E480) on the PZT film surface after sintering. In order to

Table 2
Statistical analysis of splats and clusters deposited at different working distances

Deposition distance (mm)	Spray deposition width (mm)	Size of splats (μm)				Size of clusters (μm)			
		Maximum	Minimum	Average	Standard deviation	Maximum	Minimum	Average	Standard deviation
20	23	7.7	2.7	4.2	1.4	3.0	0.3	0.6	0.4
15	17	12.5	2.7	6.2	2.4	3.0	0.3	0.6	0.4
10	12	18.0	2.7	8.0	3.0	2.5	0.3	0.5	0.3

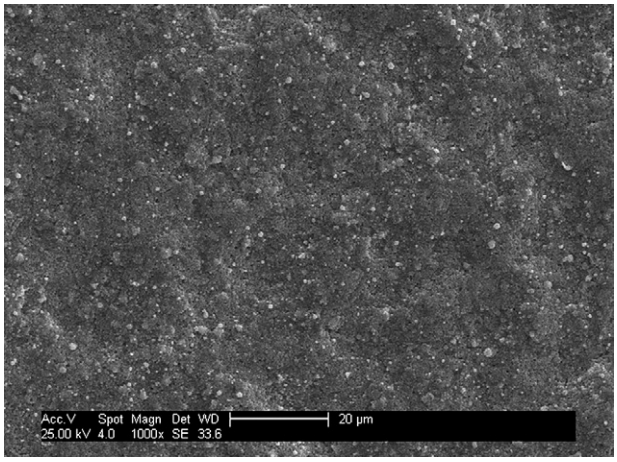

Fig. 6. Scanning electron microscope micrograph showing the microstructure of the surface of a 20 layer PZT film produced at working distance of 10 mm, a flow rate of 2.2×10^{-10} m^3 s^{-1} and an applied voltage of 5.5 kV.

examine the droplet distribution, a single quick pass deposition was carried out by setting the travelling speed of the *X–Y* stage to 30 mm s^{-1}.

3. Results and discussion

3.1. Deposition product analysis

During the EHDA process, the working distance between the needle and ground electrode is a key factor for the control of the deposition product. The electric field and EHDA jetting mode can be affected by the changes in the working distance. The deposition process with 20 mm, 15 mm and 10 mm needle exit–substrate distance (hereinafter called working distance) was carried out and examined in this work. In order to obtain a stable jet, the flow rate was kept constant at 2.2×10^{-10} m^3 s^{-1}, and the applied voltage was varied between 5.5 kV and 7.5 kV.

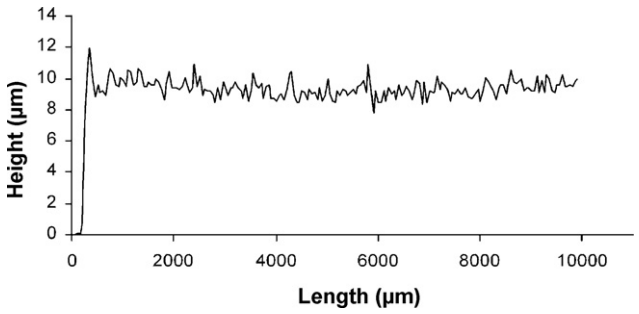

Fig. 7. Surface profile of PZT film shown in Fig. 6.

The results of a single pass deposition of this slurry at different working distances are shown in Fig. 2. The deposition product is a combination of large flattened circular splats and small spherical clusters (Fig. 2a). Splats contain well-mixed PZT powder in sol, and clusters are dry PZT particle agglomerations. The statistical analysis of the deposition results is summarized in Table 2. The influence of working distance on the size and density of splats and clusters are shown in Figs. 3 and 4, respectively. At a high working distance (20 mm) the size and number density of splats are smaller than that at low distances (15 mm and 10 mm) (Fig. 3). For the 10 mm working distance the average diameter of splats was ~8 μm, almost double that observed at 20 mm working distance (Table 2). The increase of splat size

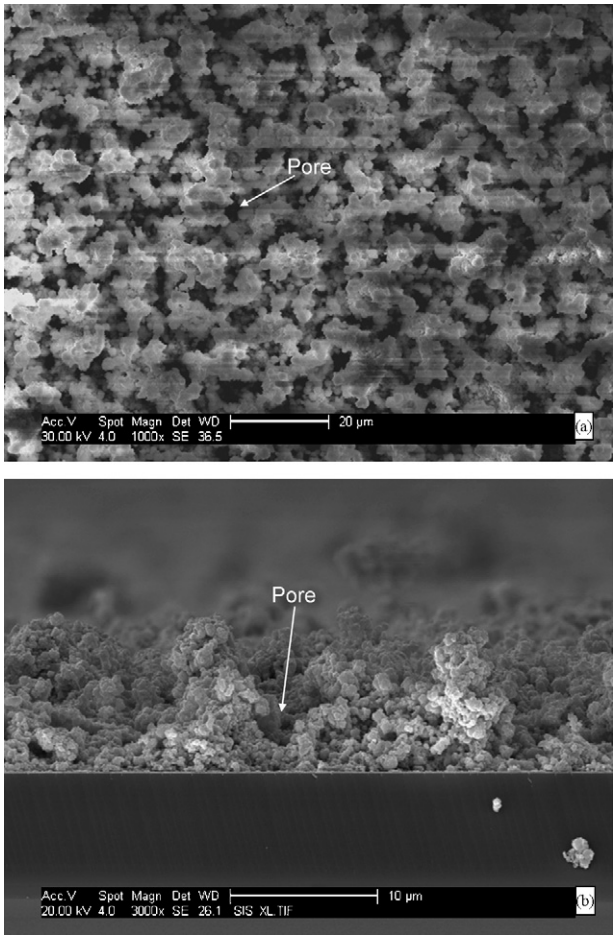

Fig. 8. Scanning electron micrographs showing the microstructure of (a) the surface and (b) the cross-section of a 20 layer PZT films produced at working distance of 20 mm, a flow rate of 2.2×10^{-10} m^3 s^{-1} and an applied voltage of 6.5 kV.

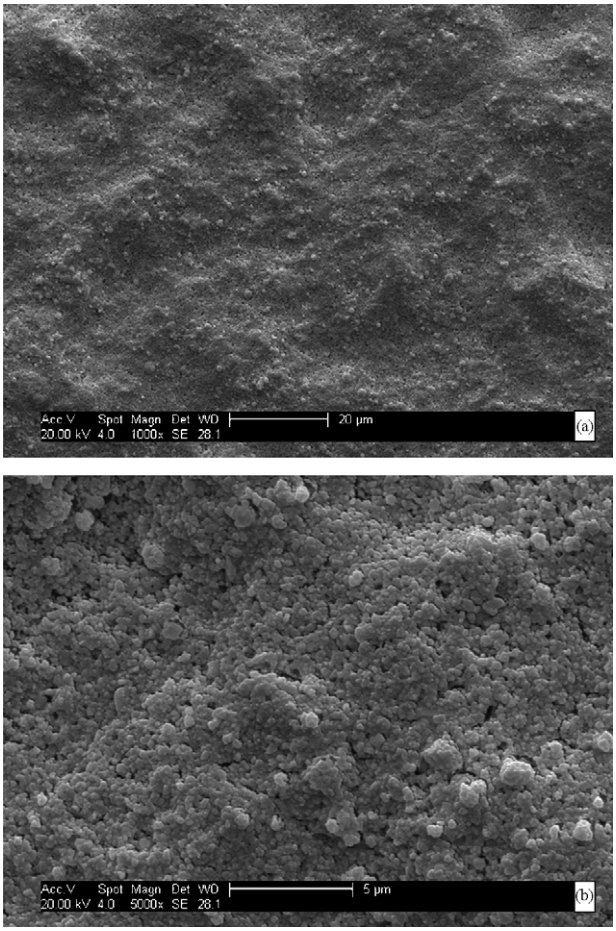

Fig. 9. Scanning electron microscope micrographs showing the microstructure of (a) the surface of a 60 layer PZT film and its (b) appearance at a high magnification. Flow rate 2.2×10^{-10} m^3 s^{-1}, applied voltage 5.5 kV and working distance 10 mm.

with the reduction of atomization distance is due to reduced droplet break-up and reduced solvent evaporation during their shorter travelling time from needle exit to substrate.

The size of clusters did not show a significant change when the working distance decreased from 20 to 15 mm (Fig. 4). The clusters produced with the working distance set at 10 mm (Fig. 2c) are slightly smaller, and the size is mostly within the range of 0.3–1.0 μm (Fig. 4), which is approximately the size of the PZT powder (mean size of ∼0.6 μm). The increasing number density of splats and clusters at a shorter working distance is due to the reduction of spray deposition area on the substrate leading to a higher flux density of droplets.

The ideal deposition products for EHDA film formation would be those with large splats and the smallest possible clusters without cracks. The use of large splats can reduce the possibility of hole generation and enhance the uniformity of the films. The clusters should be kept as small as possible because their existence can induce holes inside the films and increase the roughness of the film surface. Comparing the three working distances investigated, 10 mm with relatively larger splats and smaller clusters is closest to the ideal film build-up requirement. The 10 mm working distance between needle and ground electrode is a critical point, as the use of smaller distances increases the risk of electrical discharge between the needle and ground electrode. Therefore, this working distance of 10 mm was kept as an optimum deposition condition for forming PZT thick films using this slurry.

3.2. Formation of thick films

Fig. 5 shows a single layer deposit produced using working distances of 20 mm, 15 mm and 10 mm, respectively. The EHDA conditions were kept the same as those for one pass depositions. It can be observed that at 20 mm (Fig. 5a) more voids and bigger clusters are prevalent compared with that at 15 mm (Fig. 5b) and 10 mm (Fig. 5c). This is similar to the observation discussed in Section 3.1 where the number density of deposition products is low and the size of clusters is high at higher distances (Fig. 2). It was also found that cracks appeared in the films when multiple splats were deposited on top of each other which is due to the sol induced shrinkage stresses leading to fracture at the edges of the splats. However, the cracks were no longer evident when 20 layers were built up (Fig. 6) as the cracks were filled when the sol inside the later deposited splats infiltrates into pre-deposited layers. The surface profile of this film examined using a Surface Profiler (Veeco Instruments Incorporation, UK) is shown in Fig. 7.

The microstructure of the surface and the cross-section after 20 layer deposition at a working distance of 20 mm are shown in Fig. 8a and b, respectively, and exhibit porous features, owning to the relatively smaller splats and bigger clusters deposited under these conditions (Fig. 2a). These features can be inferred from the single layer deposition results (Fig. 5a) where existing clusters serve as an electrode for the oncoming travelling cluster and thus the moving clusters which are attracted to settle above it, resulting in the porosity.

A high density PZT film, ∼28 μm thick, was produced using 60 layers of EHDA deposition with a working distance of 10 mm. To avoid sedimentation of the slurry in the syringe, fresh slurry was used after every 20 layers of deposition (∼30 min), the needle was also cleaned at this time. To do this, deposition was stopped for 180 s. The total time to complete 60 layers of deposition was ∼96 min. The top view of this film (Fig. 9a) shows a dense and crack-free appearance despite the existence of ∼400 nm pores within the film (Fig. 9b). It is also observed that the surface of this film is uneven (Fig. 9a), which can be flattened further by smoothing the mechanical movement of *X*–*Y* stage of the EHDA printer. The cross-section of this film (Fig. 10a) shows a crack-free homogenous film. The higher magnification micrograph (Fig. 10b) shows well-packed PZT particles and submicrometer sized pores in the film. It was noted that there is a ∼1 μm thick denser PZT layer above the Pt electrode (Fig. 10c), which could be formed by the deposition of the first few layers on Pt and the infiltration of sol from subsequently deposited splats. The uniform PZT thick film was formed above this denser layer. The pores in the film were caused by the evaporation of solvent and packing of PZT grains during the drying process (Fig. 10c).

The XRD pattern of sintered films (Fig. 11) shows only the perovskite structure. The relative permittivity (ε_r) of this film was calculated to be ∼220. The low value of this property is

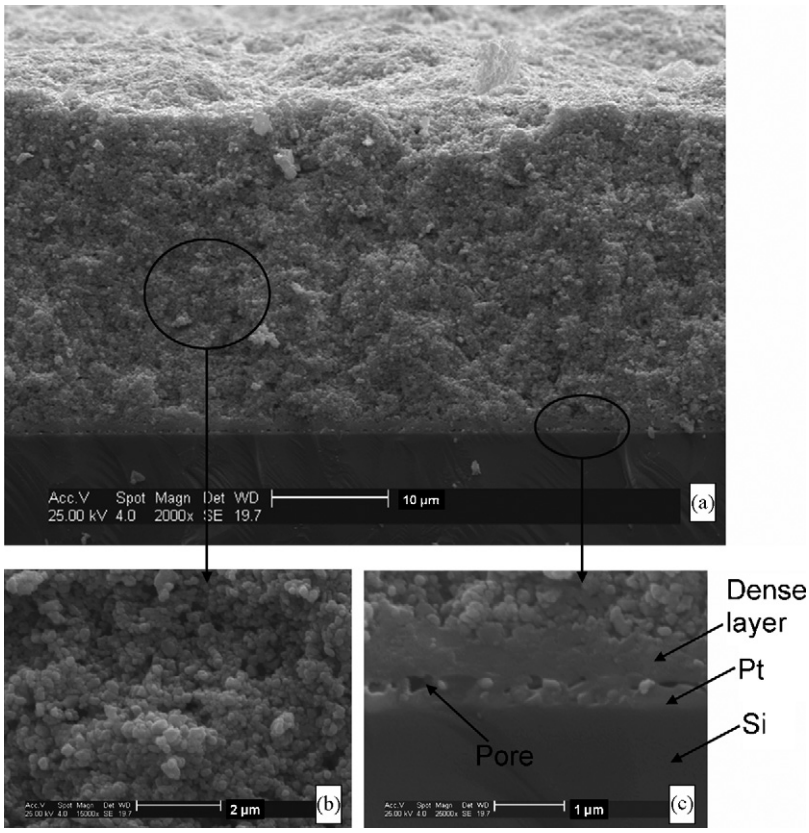

Fig. 10. Scanning electron microscope micrographs showing (a) a typical cross-section of PZT film (60 layers) on Si substrate, (b) the arrangement of PZT particles in film and (c) porous PZT/Pt/Si interfacial region.

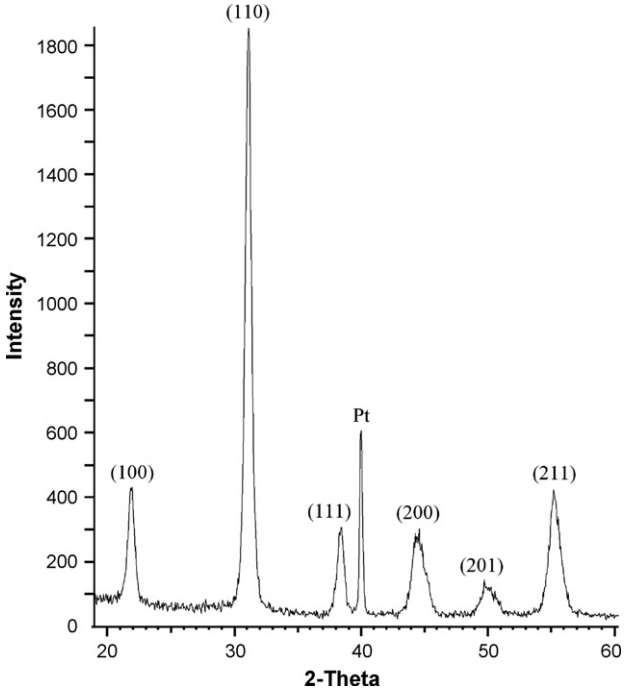

Fig. 11. X-ray pattern of the 60 layered (∼28 μm) EHDA PZT film after sintering at 720 °C for 20 min (the Pt peak observed resulted from an area of deliberately exposed bottom electrode).

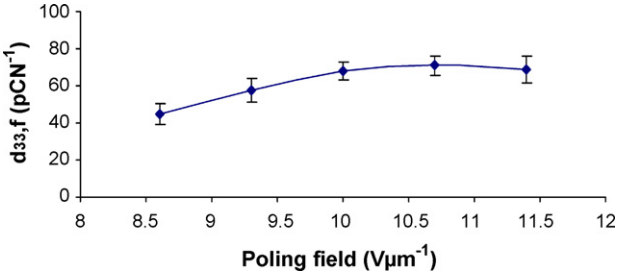

Fig. 12. Piezoelectric constant of the 60 layered (∼28 μm thick) PZT film poled at 200 °C for 5 min at different poling fields.

mainly due to the existence of pores in the PZT films. The piezoelectric constant (d_{33}) at different poling voltages is shown in Fig. 12. The highest d_{33} obtained was 71 pC N^{-1} when poled at ∼10.7 V μm^{-1} at 200 °C for 5 min.

4. Conclusions

The use of the EHDA technique for depositing a PZT composite sol–gel slurry to form thick films was aptly demonstrated. The distance between the needle exit and the substrate was shown to play an important role in deposition and the resultant microstructure. 10 mm distance was considered to be the optimum working distance for forming homogenous films using this slurry. 10 μm and 28 μm PZT thick films, which were

crack-free and with well-packed microstructures, were thus produced. The piezoelectric coefficient ($d_{33,f}$) of 71 pC N^{-1} was obtained for 28 μm thick films, which is comparable with the composite films produced using the spin-coating technique and screen printed PZT. The properties can be improved further by increasing the density and reducing the roughness of the films. The fabrication of PZT thick films using EHDA provides a new, effective and promising manufacturing route for MEMS device.

Acknowledgements

Dr. Sophie Rocks and Mr. Andrew Stallard are thanked for their generous help with this work. This work is funded by EPSRC (GR/84156/01), the European commission as part of the MIND (Multifunctional & Integrated Piezoelectric Device) project and the Piezo Institute. Dr Dorey is a Royal Academy of Engineering/EPSRc research fellow.

References

[1]. Gebhardt, S., Seffner, L., Schlenkrich, F. and Schonecker, A., PZT thick films for sensor and actuator applications. *J. Eur. Ceram. Soc.*, 2007, **27**, 4177–4180.

[2]. Kim, H., In, C., Yoon, G. and Kim, J., Design and fabrication of a micro PZT cantilever array actuator for applications in fluidic systems. *J. Mech. Sci. Technol.*, 2005, **19**, 1544–1553.

[3]. Kozielski, L., Lisinska-Czekaj, A. and Czekaj, D., Graded PZT ceramics for piezoelectric transformers. *Prog. Solid State Chem.*, 2007, **35**, 521–530.

[4]. Zhang, Q. Q., Djuth, F. T., Zhou, Q. F., Hu, C. H., Cha, J. H. and Shung, K. K., High frequency broadband PZT thick film ultrasonic transducers for medical imaging applications. *Ultrasonics*, 2006, **44**, E711–E715.

[5]. Haertling, G. H., Ferroelectric ceramics: history and technology. *J. Am. Ceram. Soc.*, 1999, **82**, 797–818.

[6]. Dorey, R. A. and Whatmore, R. W., Electroceramic thick film fabrication for MEMS. *J. Electroceram.*, 2004, **12**, 19–32.

[7]. Zhou, Q. F., Chan, H. L. W. and Choy, C. L., Conducting lanthanum nickel oxide as electrodes for lead zirconate titanate films. *Thin Solid Films*, 2000, **375**, 95–99.

[8]. Le Dren, S., Simon, L., Gonnard, P., Troccaz, M. and Nicolas, A., Investigation of factors affecting the preparation of PZT thick films. *Mater. Res. Bull.*, 2000, **35**, 2037–2045.

[9]. Mass, R., Koch, M., White, N. M. and Evans, A. G. R., Thick-film printing of PZT onto silicon. *Mater. Lett.*, 1997, **31**, 109–112.

[10]. Dorey, R. A. and Whatmore, R. W., Pyroelectric properties of PZT/PMNZTU composite thick films. *J. Electroceram.*, 2004, **12**, 191–196.

[11]. Dauchy, F. and Dorey, R. A., Patterned crack-free PZT films for micro-electromechanical system applications. *In. J. Adv. Manuf. Technol.*, 2007, **33**, 86–94.

[12]. Dauchy, F. and Dorey, R. A., Patterned high frequency thick film MEMS transducer. *Integr. Ferroelectr.*, 2007, **90**, 42–52.

[13]. Jaworek, A. and Krupa, A., Classification of the modes of EHD spraying. *J. Aerosol Sci.*, 1999, **30**, 873–893.

[14]. Zeleny, B. J., The electrical discharge from liquid points, and a hydrostatic method of measuring the electric intensity at their surfaces. *Phys. Rev.*, 1914, **3**, 69–91.

[15]. Rayleigh, L., On the equilibrium of liquid conducting masses charged with electricity. *Phil. Mag.*, 1882, **14**, 184–186.

[16]. Jayasinghe, S. N. and Edirisinghe, M. J., A novel process for simultaneous printing of multiple tracks from concentrated suspensions. *Mater. Res. Innov.*, 2003, **7**, 62–64.

[17]. Jaworek, A., Electrospray droplet sources for thin film deposition. *J. Mater. Sci.*, 2007, **42**, 266–297.

[18]. Cloupeau, M. and Prunet-Foch, B., Electrohydrodynamic spraying functioning modes: a critical review. *J. Electrostat.*, 1994, **25**, 1021–1036.

[19]. Taylor, G., Disintegration of water drops in an electric field. *Proc. R. Soc. Lond.*, 1964, **280**, 383–397.

[20]. Jone, A. R. and Thong, K. C., Production of charged monodisperse fuel droplets by electrical dispersion. *J. Phys. D-Appl. Phys.*, 1971, **4**, 1159–1161.

[21]. Ganan-Calvo, A. M., Davila, J. and Barrero, A., Current and droplet size in the electrospraying of liquids. Scaling laws. *J. Aerosol Sci.*, 1997, **28**, 249–275.

[22]. Loscertales, I. G., Barrero, A., Guerrero, I., Cortijo, R., Marquez, M. and Ganan-Calvo, A. M., Micro/nano encapsutation via electrified coaxial liquid jets. *Science*, 2002, **295**, 1695–1698.

[23]. Tay, B. Y., Evans, J. R. G. and Edirisinghe, M. J., Solid freeform fabrication of ceramics. *Int. Mater. Rev.*, 2003, **48**, 341–370.

[24]. Dorey, R. A., Stringfellow, S. B. and Whatmore, R. W., Effect of sintering aid and repeated sol infiltrations on the dielectric and piezoelectric properties of a PZT composite thick film. *J. Eur. Ceram. Soc.*, 2002, **22**, 2921–2926.

[25]. Villegas, M., Moure, C., Jurado, J. R. and Duran, P., Improvements of sintering and piezoelectric properties of soft lead zirconate titanate ceramics. *J. Mater. Sci.*, 1994, **29**, 4975–4983.